KYBERNETIKA — VOLUME *51* (2015), NUMBER 1, PAGES 4–19

A STUDY ON GLOBAL STABILIZATION OF PERIODIC ORBITS IN DISCRETE-TIME CHAOTIC SYSTEMS BY USING SYMBOLIC DYNAMICS

Masayasu Suzuki and Noboru Sakamoto

In this report, a control method for the stabilization of periodic orbits for a class of one- and two-dimensional discrete-time systems that are topologically conjugate to symbolic dynamical systems is proposed and applied to a population model in an ecosystem and the Smale horseshoe map. A periodic orbit is assigned as a target by giving a sequence in which symbols have periodicity. As a consequence, it is shown that any periodic orbits can be globally stabilized by using arbitrarily small control inputs. This work is a new attempt to systematically design a control system based on symbolic dynamics in the sense that one estimates the magnitude of control inputs and analyzes the Lyapunov stability.

Keywords: symbolic dynamics, chaos control, global stability

Classification: 37B10, 74H65, 93D15

1. INTRODUCTION

Chaos, signifying randomness and irregularity, is ubiquitous in nonlinear dynamical systems. The hallmark of chaos is sensitive dependence of the system's state on initial conditions. That is, a small error in the initial conditions can lead to a large error in the state of the system after a finite time interval. In many practical situations it is desirable if chaos can be avoided. The OGY-method was proposed as the first method controlling chaos in 1990 [7, 13], and since then, much related research has been carried out. The principal purpose of chaos control is stabilization of a periodic orbit embedded in an attractor.

Symbolic dynamics is introduced in order to characterize the orbit structure of a dynamical system via infinite sequences of "symbols" [12, 17]. The study on symbolic dynamics has a long history. The first application was shown in Hadamard's work of geodesics on surfaces of negative curvature [5]. Birkhoff used symbolic dynamics in his studies of dynamical systems [1]. Morse and Hedlund studied symbolic dynamics as an independent subject [11]. Levinson applied it for the study of the forced van der Pol equation [8], and from his result, Smale introduced the well-known horseshoe mapping [16]. In chaos engineering, symbolic dynamics is used for chaos communication [6], and

DOI: 10.14736/kyb-2015-1-0004

the targeting problem in which trajectories from initial states to the neighborhood of a target orbit are designed [2, 3, 4].

This paper is concerned with the global stabilization of a periodic orbit embedded in a chaotic trajectory. To this end, first, a control law is designed in the sequence space such that the target periodic orbit becomes asymptotically stable. Next, the control law is transformed to the state space. By the proposed method, we design a one-dimensional control system for a population model in an ecosystem, and a two-dimensional control system with one input for the Smale horseshoe map. Although we follows an idea [2, 3, 4, 6] that one evaluates the states of systems and controls them on the side of symbolic dynamics, our work is the first exposition using symbolic dynamics in order to design control systems systematically in the sense that one can estimate the magnitude of control inputs and analyze the Lyapunov stability. The use of symbolic dynamics for design is effective since it is possible to globally stabilize any periodic orbit with arbitrarily small inputs by a uniform control law that does not switch from targeting to local stabilization, which is not an easy task with the conventional state space approach.

2. SYMBOLIC DYNAMICS

2.1. Symbolic dynamics

Consider the following discrete-time dynamical system defined on $\mathbb{R}$ or $\mathbb{R}^2$ that has an invariant set X.

$$x_{n+1} = f(x_n),\ x_n \in X \subset \mathbb{R} \text{ or } \mathbb{R}^2. \tag{1}$$

Let $S = \{0, 1, \ldots, N\}$ be a set of symbols, and let $N+1$ subsets $X_0, \ldots, X_N$ be disjoint sets, the union of which is the invariant set X. That is,

$$X = X_0 \cup X_1 \cup \cdots \cup X_N,\ X_i \cap X_j = \emptyset\ \ (i \neq j)$$

holds. Furthermore, for a state $x \in X$, consider a correspondence to give the i times iteration of f, $f^i(x)$, a symbol with an index, $s_i \in S$, as follows:

$$f^i(x) \in X_k \Longrightarrow s_i = k.$$

Then, we define a set Σ as the infinite direct product of S, $\Sigma := \prod_{i=-\infty}^{\infty} S_i$, $S_i = S\ (\forall\, i)$, and a mapping $\Psi : X \to \Sigma$ by

$$\Psi(x) = \cdots s_{-2}s_{-1}\bullet s_0 s_1 s_2 \cdots,\ x \in f^{-i}(X_k).$$

Here, we add the decimal point to the sequence to indicate that the symbol lying at the right of it corresponds to the non-iterated state. Moreover, define a mapping $\sigma : \Sigma \to \Sigma$ as

$$\sigma(\cdots s_{-2}s_{-1}\bullet s_0 s_1 \cdots) = \cdots s_{-1}s_0\bullet s_1 s_2 \cdots.$$

The set Σ, for which one can give some mathematical structures in fact, is called the *sequence space*, and the mapping σ the *shift*. In this paper, we consider the following

metric between two-side infinite sequences ρ and ρ':

$$d_\Sigma(\rho, \rho') = \sum_{i=-\infty}^{\infty} \frac{1}{2^{|i|}} \frac{|s_i - s'_i|}{1 + |s_i - s'_i|}. \tag{2}$$

Denote the dynamics of the mapping f on its invariant set X as (X, f), and the dynamics of the mapping σ on Σ as (Σ, σ). When Ψ is a homeomorphic mapping and satisfies $\sigma \circ \Psi = \Psi \circ f$, the pairs (X, f) and (Σ, σ) are said to be topological conjugate, which is represented by the commutative diagram in Figure 1. Then, the system (Σ, σ) is called *symbolic dynamical system* for the system (X, f).

$$\begin{array}{ccc} X & \xrightarrow{f} & X \\ \Psi \downarrow & & \downarrow \Psi \\ \Sigma & \xrightarrow{\sigma} & \Sigma \end{array}$$

Fig. 1. The commutative diagram between the dynamical system (X, f) and the symbolic dynamical system (Σ, σ).

Remark 2.1. The study on symbolic dynamics has a history of over a century. The advantages of using symbolic dynamics are as follows. If symbolic dynamics can be introduced for a dynamical system in the state space, the description of its time evolution in the sequence space, that is, shifting symbols, is simpler than that of the original system. It is easier to focus on certain properties of a dynamical system. For example, the existence of a periodic orbit with any period can be easily proven, and it is even possible to show there is a dense orbit in the state space.

Remark 2.2. The class of dynamics to which symbolic dynamics can be introduced is large. Actually, it is known that, for dynamics satisfying the axiom A[1], the non-wandering set can be divided into finite basic sets and each of basic sets introduces Markov sub-shift[2] by Markov partition (See [14]). Many dynamics, for example, Morse-Smale system, Anosov system, DA map and horseshoe, satisfy the axiom A.

2.2. Periodic orbits and the stability

Definition 2.3. If a trajectory $\{x_0, x_1, \ldots\}$ of the dynamics (X, f) satisfies that $x_{n+T} = x_n$ for some constant $T \in \mathbb{N}$, the trajectory is called a *T-periodic orbit* or simply *periodic orbit*. Then, each point of the T-periodic orbit is called a *T-periodic point* or simply *periodic point*.

[1] A diffeomorphism $f : M \to M$ (M is a manifold) such that the non-wandering set $\Omega(f)$ is hyperbolic and a set of all periodic points $Per(f)$ is dense in $\Omega(f)$, is said to satisfy axiom A.

[2] Markov sub-shift is a restriction of the shift σ to Σ_A, where $\Sigma_A \subset \Sigma$ is a σ-invariant subset given by a transition matrix describing how sequences evolve.

We find that a state $x \in X$ is a T-periodic point if and only if the sequence $\rho \in \Sigma$ corresponding to x consists of infinitely repeated T-length blocks of symbols.

$$\rho = \Psi(x) = \cdots \underbrace{s_1 s_2 \cdots s_T}_{T\text{-length block}} \underbrace{s_1 s_2 \cdots s_T}_{T\text{-length block}} \cdots,$$

which means that all periodic orbits in the invariant set can be specified by periodic sequences.

In this paper, we describe a periodic point in X and the corresponding sequence in Σ by adding " $\bar{}$ ", as $\bar{x}$ and $\bar{\rho} = \Psi(\bar{x}) = \cdots \bar{s}_0 \bar{s}_1 \cdots$, respectively. Furthermore, denote a T-periodic orbit by a finite set $\gamma_T = \{\bar{x}_0, \bar{x}_1, \ldots, \bar{x}_{T-1}\}$, and let $\mathcal{P}_T$ be a set of the sequences corresponding to γ_T as follows:

$$\mathcal{P}_T = \{\bar{\rho}_0, \bar{\rho}_1, \ldots, \bar{\rho}_{T-1}\},\ \bar{\rho}_i = \Psi(\bar{x}_i),\ i = 1, 2, \ldots, T.$$

We define the distance between a state $x \in X$ and a periodic orbit $\gamma_T \subset X$ by $d^*(x, \gamma_T) := \min_{y \in \gamma_T} d(x, y)$, where d is some metric in X. Then, we consider the following stability of a periodic orbit in the sense of Lyapunov.

Definition 2.4. A periodic orbit γ_T is said to be stable if, for all $\varepsilon > 0$, there exists a $\delta = \delta(\varepsilon) > 0$ such that, for any solution $\{f^n(x_0)\}$ satisfying $d^*(x_0, \gamma_T) < \delta$, we have $d^*(f^n(x_0), \gamma_T) < \varepsilon$ for all $n \geq 0$. A periodic orbit is said to be unstable if it is not stable.

Definition 2.5. A periodic orbit γ_T is said to be globally asymptotically stable if it is stable and, for any initial state x_0, we have $\lim_{n \to \infty} d^*(f^n(x_0), \gamma_T) = 0$.

3. DESIGN OF A CONTROL SYSTEM BASED ON SYMBOLIC DYNAMICS

Now, let us consider the following control system for system (1).

$$x_{n+1} = f(x_n) + u_n. \tag{3}$$

We formulate the problem to be tackled in this paper as follows:

Problem Design a control law u_n in (3) that globally stabilizes the unstable periodic orbit γ_T in system (1). Furthermore, design a control law that accomplishes the stabilization of γ_T with inputs whose magnitudes are less than a value given arbitrarily.

3.1. Control law in the sequence space

In the sequence space Σ, the time evolution of sequences by the shift mapping σ is described as

$$\rho_{n+1} = \sigma(\rho_n).$$

Here, ρ_n is the sequence corresponding to the state x_n, i. e. $\rho_n = \Psi(x_n)$. To address the above problem, we first design a control law in the sequence space Σ, which means to

alter σ so that an orbit starting at an arbitrary initial sequence ρ_0 converges to $\mathcal{P}_T \subset \Sigma$ corresponding to $\gamma_T \subset X$. Due to the metric of (2) in Σ, we notice that the more symbols from the decimal point toward both sides agree in ρ and ρ', the closer ρ and ρ' are. Therefore, a new σ, which we denote as π, requires rewriting symbols in the sequence. Let k and l be integers with $k \geq 0$ and $l \geq 1$, respectively. Assume that each of the T-periodic sequences in $\mathcal{P}_T$ consists of infinitely repeated T-length block $P_T = r_1 r_2 \cdots r_T$. The mapping of the new closed-loop system,

$$\rho_{n+1} = \pi(\rho_n) \tag{4}$$

should have the following time evolution.

$$\begin{aligned}
\rho &= \cdots{}_\bullet s_0 \cdots s_{k-1} s_k \quad \cdots s_{k+l-2} s_{k+l-1} \cdots s_{k+2l-3} \cdots, \\
\pi(\rho) &= \cdots{}_\bullet s_1 \cdots \underline{\bar{s}_k \quad \bar{s}_{k+1} \cdots \bar{s}_{k+l-1}} s_{k+l} \quad \cdots s_{k+2l-2} \cdots, \\
\pi^2(\rho) &= \cdots{}_\bullet s_2 \cdots \bar{s}_{k+1} \bar{s}_{k+2} \cdots \underline{\bar{s}_{k+l} \quad \bar{s}_{k+l+1} \cdots \bar{s}_{k+2l-1}} \cdots, \\
&\vdots \qquad\qquad\qquad\qquad \vdots
\end{aligned} \tag{5}$$

The above underlined blocks of l-length consist of a part of P_T or several P_T's with its part. The parameter k is the place that the target symbols are inserted in. The parameter l is the length of the inserted target symbols. As a consequence, the orbit $\{\pi^n(\rho)\}_{n=0}^{\infty}$ converges to $\mathcal{P}_T$.

$$d_\Sigma^*(\pi^n(\rho), \mathcal{P}_T) \to 0 \ (n \to \infty)$$

where $d_\Sigma^*(\rho, \mathcal{P}_T) = \min_{\xi \in \mathcal{P}_T} d_\Sigma(\rho, \xi)$. The following proposition gives us the specific description of the mapping π.

Proposition 3.1. The mapping π in (5) can be denoted as a composition of the shift mapping σ and a mapping $\phi : \Sigma \to \Sigma$ as follows:

$$\pi = \phi \circ \sigma.$$

Proof. We prove the existence of such a mapping ϕ constructively. Consider a sequence $\rho = \cdots s_{-1} {}_\bullet s_0 s_1 \cdots$. Let $\bar{\rho} = \cdots \bar{s}_{-1} {}_\bullet \bar{s}_0 \bar{s}_1 \cdots$ be the closest sequence to ρ in $\mathcal{P}_T$. Furthermore, let m be larger than k and satisfy, for $k+1 \leq i \leq m-1$, $s_i = \bar{s}_i$, and $s_m \neq \bar{s}_m$. We define a rewriting mapping $\phi : \Sigma \to \Sigma$ such that l-length block L, that consists of l symbols from $(m+1)$-th symbol in $\bar{\rho}$, is inserted between m-th and $(m+1)$-th symbols in ρ which mean s_{m-1} and s_m, respectively. That is, we define ϕ as follows: For two sequences

$$\begin{aligned}
\bar{\rho} &= \cdots{}_\bullet \bar{s}_0 \bar{s}_1 \cdots \bar{s}_k \underbrace{\bar{s}_{k+1} \cdots \bar{s}_{m-1}}_{\|} \overbrace{\underbrace{\bar{s}_m}_{\nparallel} \bar{s}_{m+1} \cdots \bar{s}_{m+l-1}}^{l\text{-length block } L} \cdots, \\
\rho &= \cdots{}_\bullet s_0 s_1 \cdots s_k \overbrace{\bar{s}_{k+1} \cdots \bar{s}_{m-1}} \ \overbrace{s_m} \ s_{m+1} \cdots, \\
&\qquad\qquad\qquad\qquad \uparrow \text{ insert the } l\text{-length block } L
\end{aligned}$$

the image of ρ by ϕ is

$$\phi(\rho) = \cdots {}_{\bullet} s_0 s_1 \cdots s_k \bar{s}_{k+1} \cdots \bar{s}_{m-1} \underline{\bar{s}_m \bar{s}_{m+1} \cdots \bar{s}_{m+l-1}} \cdots .$$

Then, the composition of ϕ and σ gives the time evolution as (5). □

3.2. Control law in the state space

In the sequence space Σ, rewriting a sequence means controlling the time evolution of the sequence. Now, we design a control law in the state space X to realize the closed-loop system (4) in Σ. We define a new mapping $\tilde{f}$, instead of f in (1), corresponding to the mapping π as Figure 2.

$$\begin{array}{ccc} \Sigma & \xrightarrow{\pi} & \Sigma \\ {\scriptstyle \Psi^{-1}}\downarrow & & \downarrow{\scriptstyle \Psi^{-1}} \\ X & \xrightarrow{\tilde{f}} & X \end{array}$$

Fig. 2. A mapping $\tilde{f}$ in X corresponding to π in Σ.

The closed-loop system in the state space is induced from π as follows:

$$x_{n+1} = f(x_n) + u(x_n), \tag{6}$$

where

$$\begin{aligned} u(x) &= \tilde{f}(x) - f(x), \\ \tilde{f}(x) &= (\Psi^{-1} \circ \pi \circ \Psi)(x). \end{aligned}$$

The input $u_n = u(x_n)$ is the function of the state x_n, therefore, system (6) is a state feed-back system (See Figure 3). The design parameter k, which specifies the position of the modification of symbols, dominates the magnitude of the inputs in the sense that the magnitude of the inputs can be smaller by choosing a larger k. Also, the design parameter l, which is the length of the modified symbols, dominates the convergence rate of $\pi^n(\rho)$ (See the next section).

Remark 3.2. The number of the inputs of the above control system does not necessarily have to be equal to the dimension of the state space X. The state space of a chaotic system with hyperbolic structure is stretched and compressed at the same time, as shown in the Smale horseshoe map (9) and (10) in Section 5.3. For such a dynamical system, since rewriting symbols in the right-hand side of the decimal point corresponds to controlling the system so as to transfer the state in the direction in which X is stretched, one does not need the inputs in the compression direction of X. Therefore, it may be accomplished to stabilize periodic orbits by a small number of inputs if the directions of the inputs transversely intersects with the compression directions, as shown in the two-dimensional system with one input (11) in Section 5.3.

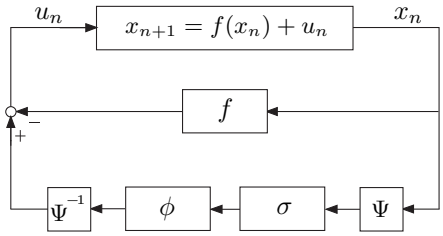

Fig. 3. The state feed-back system.

4. AN ESTIMATION OF THE MAGNITUDE OF THE CONTROL INPUTS AND THE STABILITY ANALYSIS

In this section, for the feedback system (6), we estimate the magnitude of the inputs, and analyze the stability of periodic orbits.

4.1. An estimation of the magnitude of the control inputs

To stabilize a periodic orbit of the original system (1), the feedback system (6) must also have the same periodic orbit. The following proposition guarantees it.

Proposition 4.1. The T-periodic orbit γ_T in dynamics (X, f) is also a T-periodic orbit in the feedback systems (6). Moreover, $u|_{\gamma_T} = 0$.

Proof. Suppose that a state x_n coincides with a periodic point $\bar{x}_n \in \gamma_T$. Since $\pi = \sigma$ on $\mathcal{P}_T$, we have $(\pi \circ \Psi)(x_n) = (\sigma \circ \Psi)(x_n)$. Therefore, we get $\tilde{f}(x_n) = f(x_n)$ and $u_n = u(x_n) = 0$. Since $x_{n+1} = f(x_n) + u_n = f(\bar{x}_n)$, it turns out that $x_{n+1} = \bar{x}_{n+1} \in \gamma_T$. □

Furthermore, we have the theorem concerning the magnitude of the inputs of (6).

Theorem 4.2. For all $\varepsilon > 0$, there exists a $K = K(\varepsilon) > 0$ such that if the design parameter k is larger or equal to K, then we have $\|u_n\| < \varepsilon$ for all $n \geq 0$.

Proof. The sequences corresponding to $\tilde{f}(x_n)$ and $f(x_n)$ are

$$\tilde{\rho}_{n+1} := \Psi(\tilde{f}(x_n)) = \underbrace{\cdots s_n}_{\|} \bullet \underbrace{s_{n+1}s_{n+2}\cdots s_{n+k}}_{\|} \bar{s}_{n+k+1}\cdots$$

$$\rho_{n+1} := \Psi(f(x_n)) = \overbrace{\cdots s_n} \bullet \overbrace{s_{n+1}s_{n+2}\cdots s_{n+k}}\, s_{n+k+1}\cdots,$$

respectively, that is, all left symbols and at least k right symbols from the decimal point in two sequences agree. From the metric in Σ, it turns out that $d_\Sigma(\tilde{\rho}_{n+1}, \rho_{n+1}) < 1/2^{k-1}$. Since Ψ^{-1} is continuous, the smaller the distance between $\tilde{\rho}_{n+1}$ and ρ_{n+1} is, the smaller the distance between $\tilde{f}(x_n)$ and $f(x_n)$ is. Therefore, given $\varepsilon > 0$, there exists a δ such that, if $d_\Sigma(\tilde{\rho}_{n+1}, \rho_{n+1}) < \delta$, then $d(\tilde{f}(x_n), f(x_n)) < \varepsilon$. If we choose k such that $k > \log_2(1/\delta) + 1$, then $d_\Sigma(\tilde{\rho}_{n+1}, \rho_{n+1}) < \delta$, and thus, we have $\|u_n\| < \varepsilon$. □

4.2. The stability analysis of periodic orbits

In order to analyze the stability of periodic orbits of the feedback system (6), we define the neighborhood V_j of a sequence ρ in Σ by

$$V_j(\rho) := \{\tilde{\rho} \in \Sigma | \tilde{s}_i = s_i,\ |i| < j\}.$$

For an integer j and a periodic orbit $\gamma_T = \{\bar{x}_0, \bar{x}_1, \ldots, \bar{x}_T\}$, we define a maximum radius ε_j of a neighborhood of γ_T by

$$\varepsilon_j := \max_{0 \le n \le T-1} \sup_{\rho \in V_j(\bar{\rho}_n)} d(\Psi^{-1}(\rho), \bar{x}_n),$$

where $\bar{\rho}_n = \Psi(\bar{x}_n)$. We have the following Lemma.

Lemma 4.3. For all integer j, ε_j exists. If $j' \ge j$, then $\varepsilon_{j'} \le \varepsilon_j$. Furthermore, we have $\lim_{j\to\infty} \varepsilon_j = 0$.

For the feedback system (6), we can prove the following theorem.

Theorem 4.4. Let $l \ge 2$. Then, γ_T is globally asymptotically stable.

P r o o f. From Proposition 4.1, it is proven that γ_T is a periodic orbit in the feedback system (6).

For given $\varepsilon > 0$ and $k \ge 0$, let $\delta = \min\{\varepsilon, 1/2^{k+1}\}$. For $\bar{\rho} = \cdots \bar{s}_0 \bar{s}_1 \cdots \in \mathcal{P}_T$, if $\rho = \cdots s_0 s_1 \cdots$ satisfies $d_\Sigma(\rho, \bar{\rho}) < \delta$, then we have

$$s_i = \bar{s}_i,\ |i| \le \eta,$$

where η is the largest integer less than or equal to $\max\{\log_2(1/\varepsilon) - 1, k\}$. Since some symbols in $\pi(\rho)$ and $\pi(\bar{\rho})$ agree as follows,

$$\pi(\rho) = \cdots \underbrace{\bar{s}_{-\eta} \cdots \bar{s}_0}_{\|} \bullet \underbrace{\bar{s}_1 \bar{s}_2 \cdots \bar{s}_\eta}_{\|} \underbrace{\bar{s}_{\eta+1} \cdots \bar{s}_*}_{\|} s_{*+1} \cdots$$

$$\pi(\bar{\rho}) = \cdots \overbrace{\bar{s}_{-\eta} \cdots \bar{s}_0}^{\uparrow} \bullet \overbrace{\bar{s}_1 \bar{s}_2 \cdots \bar{s}_\eta}^{\uparrow} \overbrace{\bar{s}_{\eta+1} \cdots \bar{s}_*}^{\uparrow} \bar{s}_{*+1} \cdots .$$

$(\eta+1)$-length $\quad$ η-length $\quad$ more than l-length

it turns out

$$d_\Sigma(\pi(\rho), \pi(\bar{\rho})) < d_\Sigma(\rho, \bar{\rho}) < \delta.$$

Therefore, we have

$$d_\Sigma(\pi^n(\rho), \pi^n(\bar{\rho})) < \delta \le \varepsilon,\ n \ge 0.$$

Note that, for a sequence ρ, if a periodic sequence $\bar{\rho}_i$ is the closest to ρ in $\mathcal{P}_T$, then $\pi(\bar{\rho}_i)$ is the closest to $\pi(\rho)$ in $\pi(\mathcal{P}_T)$. Therefore, it turns out that, if $d^*_\Sigma(\rho, \mathcal{P}_T) < \delta$, then $d^*_\Sigma(\pi^n(\rho), \mathcal{P}_T) < \varepsilon$ for all $n \ge 0$.

By the continuity of Ψ^{-1}, we prove that, for all $\lambda > 0$, there exists a $\varepsilon = \varepsilon(\lambda) > 0$ such that, if $d^*_\Sigma(\pi^n(\Psi(x)), \mathcal{P}_T) < \varepsilon$, then $d^*(\Psi^{-1}(\pi^n(\Psi(x))), \gamma_T) = d^*(\tilde{f}^n(x), \gamma_T) < \lambda$. Similarly, by the continuity of Ψ, it turns out that, for all $\delta > 0$, there exists a $\nu = \nu(\delta) > 0$ such that, if $d^*(x, \gamma_T) < \nu$, then $d^*_\Sigma(\Psi(x), \mathcal{P}_T) < \delta$. Therefore, one concludes that, for all $\lambda > 0$, there exists a $\nu > 0$ such that, if $d^*(x, \gamma_T) < \nu$, then we have $d^*(\tilde{f}^n(x), \gamma_T) < \lambda$. The stability of γ_T is proven.

The global asymptotic stability is proven as follows. For an arbitrary initial state x_0, the sequence at time $n(\geq k)$, $\pi^n(\Psi(x_0))$, has $k + n(l-1)$ $(=: j_n)$ symbols from the left being equal to those of a periodic sequence in $\mathcal{P}_T$. Therefore, a state x_n satisfies that $d^*(x_n, \gamma_T) \leq \varepsilon_{j_n}$. Since $\lim_{n\to\infty} j_n = \infty$, we have $\lim_{n\to\infty} \varepsilon_{j_n} = 0$. Therefore, it turns out that, for an arbitrary initial state $x_0 \in X$, we have $\lim_{n\to\infty} d^*(x_n, \gamma_T) = 0$. □

5. APPLICATION EXAMPLES

In this section, we show application examples of the proposed method.

5.1. A modification of the control law for calculation

Since it is difficult for calculation to treat infinite-length sequences, we modify the feedback system (6). For a state $x \in X$ and the corresponding sequence $\Psi(x)$, consider a finite-length subsequence in $\Psi(x)$ consisting of l symbols rewritten by π and centered $(2m+1)$ symbols: $s_{-m} \cdots s_{-1\bullet} s_0 s_1 \cdots s_m \underline{s_{m+1} \cdots s_{m+l}}$ (underline: the rewritten l symbols). Denote this correspondence from x to the subsequence as $\hat{\Psi}$. And also, for a finite-length sequence $\hat{\rho} = \hat{s}_{-p} \cdots \hat{s}_{-1\bullet} \hat{s}_0 \cdots \hat{s}_q$, consider a set of infinite-length sequences having $\hat{\rho}$ as a subsequence:

$$S_{\hat{\rho}} = \{\rho_l^* \hat{\rho} \rho_r^* \in \Sigma \mid \rho_l^* \text{ and } \rho_r^* \text{ are arbitrary left- and right-side infinite-length sequences, respectively}\},$$

and a mapping giving an interior point of a set $\Psi^{-1}(S_{\hat{\rho}}) \subset X$ for $\hat{\rho}$, which is denoted as $\hat{\Psi}^*$. The interior point can be chosen arbitrarily. Furthermore, for finite-length sequences, define $\hat{\sigma}$ and $\hat{\phi}$ by

$$\hat{\sigma}(s_{-p} \cdots s_{-1\bullet} s_0 s_1 \cdots s_q) = s_{-p} \cdots s_{-1} s_{0\bullet} s_1 \cdots s_q$$
$$\hat{\phi}(s_{-(m+1)} \cdots s_{-1\bullet} s_0 \cdots \underline{s_m \cdots s_{m+l-1}}) = s_{-(m+1)} \cdots s_{-1\bullet} s_0 \cdots \underline{\bar{s}_m \cdots \bar{s}_{m+l-1}},$$

and let $\hat{\pi} = \hat{\phi} \circ \hat{\sigma}$. By replacing $\tilde{f}$ of the feedback system (6) with $\hat{f} = \hat{\Psi}^* \circ \hat{\pi} \circ \hat{\Psi}$, the feedback law is realized on a calculator. We can prove that the control performance confirmed in Section 4 remains the same after this modification.

Remark 5.1. The distance between x_n and γ_T converges to 0 more rapidly by choosing larger l. $l \geq 2$ means, however, the calculation amount is getting larger actually. If one wants to avoid it, one has to let $l = 1$. We note that, although the asymptotic stability cannot be guaranteed for $l = 1$, the states can keep in a narrow tube around the periodic orbit by choosing reasonably large k.

5.2. Control of an ecosystem

One of the simplest systems an ecologist can study is seasonally breeding populations in which generations do not overlap [10]. For example, many natural populations such as temperate zone insects are of this kind. Such a relationship is expressed by a discrete-time system $x_{n+1} = f(x_n)$ (variable x_n is the magnitude of the population). There are other examples expressed in this form, as, for example, in biology the theory of genetics and epidemiology. In economics the models for the relationship between commodity quantity and price and for the theory of business cycles. In sociology, the theory of learning and the propagation of rumors in variously structured societies are described by this kind of equation. In many of these contexts, and for biological populations in particular, there is a tendency for the variable x_n to increase from one generation to the next when it is small, and for it to decrease when it is large. The discrete-time system below is a model representing such a tendency.

$$x_{n+1} = rx_n(1 - x_n),\ x_n \in [0, 1]. \tag{7}$$

This system is called *Logistic map*, and known to show chaotic behavior by choosing parameter r suitably. In particular, when $r = 4$, the system generates chaos [14], and the closed interval $[0, 1]$ is an invariant set. Furthermore, divide the interval $[0, 1]$ into two regions with the boundary value $1/2$ and give symbols "0" and "1" to the regions, respectively. That is, denote these regions as $X_0 = [0, 1/2)$, $X_1 = [1/2, 1]$. Then, symbolic dynamics (Σ, σ) can be introduced into the system (7) with $r = 4$. Here, sequences are one-side infinite sequences because (7) is not invertible. However, since the control law rewrites symbols being located on right side from the decimal point, our control method can be applied to this system (7).

Now, by adding or removing individuals in (7), we try to fluctuate the population of the individuals periodically. In particular, it is intended that the magnitude of the population always returns to the initial magnitude every 3 generations. For such a purpose, we give a 3-periodic sequence repeating "011" as a target orbit and design a control system by using the proposed method. The simulation results are shown below. Figure 4 illustrates the time evolution of the state starting at the initial condition $x_0 = 0.3$ with no control. That is, a chaotic behavior can be observed.

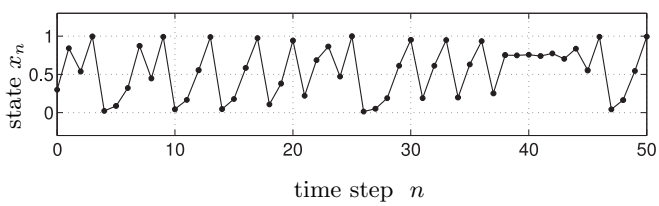

Fig. 4. Time evolution of the state without control input; initial condition $x_0 = 0.3$.

Figure 5 (a) shows the time evolutions of the states starting at the same initial condition $x_0 = 0.3$ with the design parameters $(k, l) = (1, 2)$. For the state value

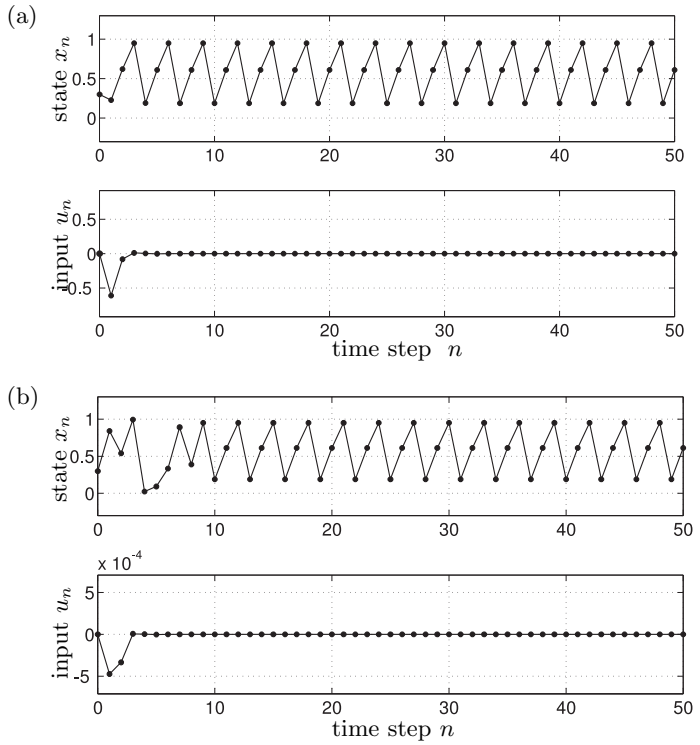

Fig. 5. Stabilization of a 3-periodic orbit embedded in a Logistic map; initial condition $x_0 = 0.3$: (a) design parameter $k = 1$, $l = 2$; (b) design parameter $k = 10$, $l = 2$.

$x_0 = 0.3$, the corresponding finite sequence, where we consider sequences of 10 symbols to explain the proposed procedure, is $\hat{\rho} = \hat{\Psi}(x_0) = {}_\bullet s_0 s_1 \cdots s_9 = {}_\bullet 0111000101$ because we have $f(x_0) = 0.84$, $f^2(x_0) = 0.5376$, $f^3(x_0) = 0.9943$, $f^4(x_0) = 0.0225$, and so on. Then the sequence $\hat{\rho}$ is shifted as $0_\bullet 111000101$. However, since the symbol at the left of the decimal point has no meaning for controlling this system, one can omit it. Therefore we treat the shift as truncation, that is, $\hat{\sigma}(\rho) = {}_\bullet s_1 s_2 \cdots s_9 = {}_\bullet 111000101$. Next we compare the truncated sequence with a periodic sequence $\bar{\rho} = {}_\bullet 011011\cdots$. Since $k = 1$, subsequence $s_2 s_3 \cdots s_9 = 11000101$ is compared to the periodic sequence $\bar{\rho}$ in turn from the left symbol. We find that s_2 disagrees, and hence, $l(= 2)$ symbols "01" in $\bar{\rho}$ is inserted between s_1 and s_2. This is the rewriting operation: $\hat{\phi}({}_\bullet 111000101) = {}_\bullet 1\underline{01}1100010$. Denote this rewritten sequence as $\check{\rho} = {}_\bullet \check{s}_0 \check{s}_1 \cdots \check{s}_9$. Then we calculate the inverse image of the rewritten sequence under $\hat{\Psi}$, $\hat{\Psi}^{-1}(\check{\rho}) = \{x \in \mathbb{R} \mid f^i(x) \in X_{\check{s}_i},\ i = 0, 1, \ldots, 9\}$, which is derived by solving simultaneous inequalities. For the system of (7), the inverse image is always an connected interval: For the above sequence, it is $[0.1464, 0.3087]$ [3].

[3] The shown numerical values are rounded.

Finally, we choose an interior point in the inverse image and calculate an input value. We here assign the midpoint of the interval as the interior point, which is denoted by x^*: For the above interval, it is $x^* = 0.2276$. Therefore the mapping $\hat{\Psi}^*$ is defined as the correspondence $\check{\rho} \mapsto x^*$ and, $\hat{f}$ $(:= \hat{\Psi}^* \circ \hat{\phi} \circ \hat{\sigma} \circ \hat{\Psi})$ as $x_0 \mapsto x^*$. For each time k, the above procedures are performed against the current state x_k instead of x_0. Note that the periodic sequence compared at the rewriting step is time-variant, that is, it is chosen from $\{\bar{\rho}, f(\bar{\rho}), f^2(\bar{\rho})\}$ in turn. It is also reasonable to choose the nearest one to the corresponding sequence, where this choice is can be said to be state-depended rather than time-depended. In Figure 5 (a), the state values (the magnitude of the population) are plotted in the top figure and the input values are plotted in the bottom figure, respectively.

Figure 5 (b) shows the simulation results with $(k, l) = (10, 2)$. From Figures 5 (a) and (b), it is confirmed that the states converge to the 3-periodic orbit. Furthermore, by comparing Figures 5 (a) and (b), it can be verified that the system with the input magnitude parameter $k = 10$ has smaller input values than those of the system with $k = 1$.

5.2.1. Comparison with the OGY-method

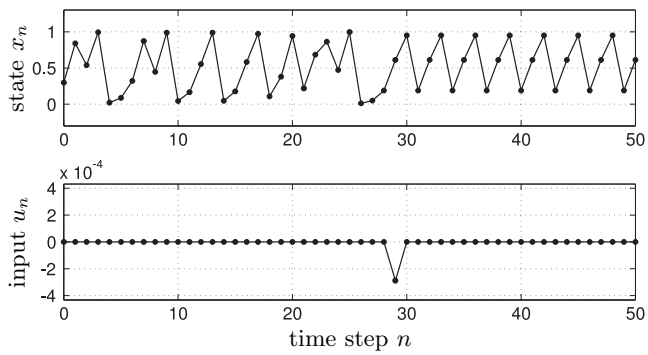

Fig. 6. Stabilization of a 3-periodic orbit embedded in Logistic map with the OGY-method; initial condition $x_0 = 0.3$.

In the OGY-method [13], the control inputs are added so that trajectories transit onto a local stable manifold, only when the state enters in a control region given in advance. The waiting time is derived statistically, and, in general, the smaller the control region is, the longer the time is. In our method, however, one can clearly know when the state will enter the neighborhood of the target even if it is small.

Figure 6 illustrates a simulation result of stabilization of the 3-periodic orbit by applying the OGY-method. The control region is a neighborhood of the 3-periodic orbit with a radius 0.001. It can be verified that it takes longer time to stabilize the 3-periodic orbit than the proposed control method.

5.2.2. A simulation of the feedback system with noise

For the logistic map (7), we consider a feedback system with white Gaussian noise $\{v_n\}$ as follows.

$$x_{n+1} = f(x_n) + u(x_n) + v_n. \tag{8}$$

We set the mean and the standard deviation of noise as $\{v_n\}$ to 0 and 10^{-4}, respectively, and simulate (8) in the case when (i) $k = 5$, $l = 2$ and (ii) $k = 10$, $l = 2$. Figure 7 shows the time evolutions of the states in these cases.

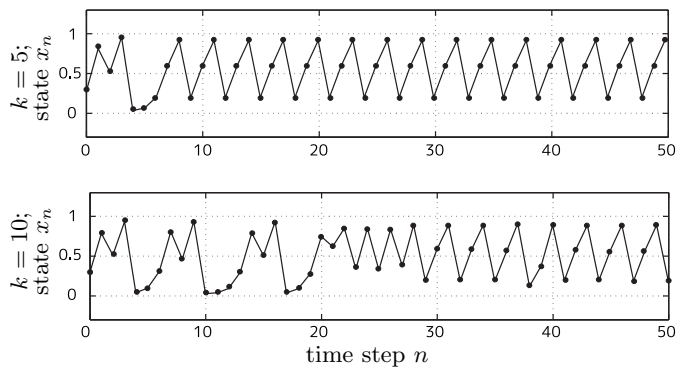

Fig. 7. Responses of the feedback system with white Gaussian noise: (i) Top figure; design parameter $k = 5$, $l = 2$: (ii) Bottom figure; design parameter $k = 10$, $l = 2$.

From Figure 7, it turns out that, the 3-periodic orbit is stabilized in the case (i), but it is not done in the case (ii). One concludes that, if the design parameter k is not sufficiently small, that is, the upper limit of the inputs is not sufficiently large, to remove the effect of the noise, then periodic orbits in (6) cannot be stabilized.

5.3. Control of the Smale horseshoe map—two-dimensional system with one input

Smale horseshoe map was introduced as the first example of diffeomorphism that had an infinite number of periodic points and were structurally stable [16]. Furthermore, understanding of the Smale horseshoe is absolutely essential for understanding what is meant by term "chaos".

Consider a square $D = [0, 1] \times [0, 1]$ on the plane, and the subsets $H_0 = [0, 1] \times [0, 1/\mu]$ and $H_1 = [0, 1] \times [1 - 1/\mu, 1]$, where $\mu > 2$. The simplified Smale horseshoe map is given

as follows [17].

$$\begin{bmatrix} x_{n+1} \\ y_{n+1} \end{bmatrix} = f(x_n, y_n), \tag{9}$$

$$f(x,y) = \begin{cases} \begin{bmatrix} \lambda & 0 \\ 0 & \mu \end{bmatrix} \begin{bmatrix} x \\ y \end{bmatrix}, & \begin{bmatrix} x \\ y \end{bmatrix} \in H_0, \\ \begin{bmatrix} -\lambda & 0 \\ 0 & -\mu \end{bmatrix} \begin{bmatrix} x \\ y \end{bmatrix} + \begin{bmatrix} 1 \\ \mu \end{bmatrix}, & \begin{bmatrix} x \\ y \end{bmatrix} \in H_1 \end{cases} \tag{10}$$

where $\lambda < 1/2$ and H_0, H_1 are compressed in the direction of x-axis and stretched in the direction of y-direction. This system (9) has an invariant set $\Lambda_{\lambda,\mu} = \{(x,y) \mid f^k(x,y) \in D, \ ^\forall k \in \mathbb{Z}\}$, which is known to be a Cantor set. Let $X_0 = H_0 \cap \Lambda_{\lambda,\mu}$ and $X_1 = H_1 \cap \Lambda_{\lambda,\mu}$. Then, symbolic dynamics can be introduced.

For the system (9) with $\mu = 3$ and $\lambda = 1/3$, we try to stabilize a 4-periodic orbit in $\Lambda_{1/3,3}$ by the following two-dimensional control system with one input:

$$\begin{bmatrix} x_{n+1} \\ y_{n+1} \end{bmatrix} = f(x_n, y_n) + \begin{bmatrix} 0 \\ 1 \end{bmatrix} u_n \tag{11}$$

where u_n is a scalar function. We give a 4-periodic sequence repeating "0011" as a target orbit. Figure 8 shows the time evolutions of the states and the inputs with the initial value $(x_0, y_0) = (1/9, 1/9) \in \Lambda_{1/3,3}$ and the design parameter $(k, l) = (5, 2)$. From Figure 8, it is confirmed that states converge to 4-periodic orbit.

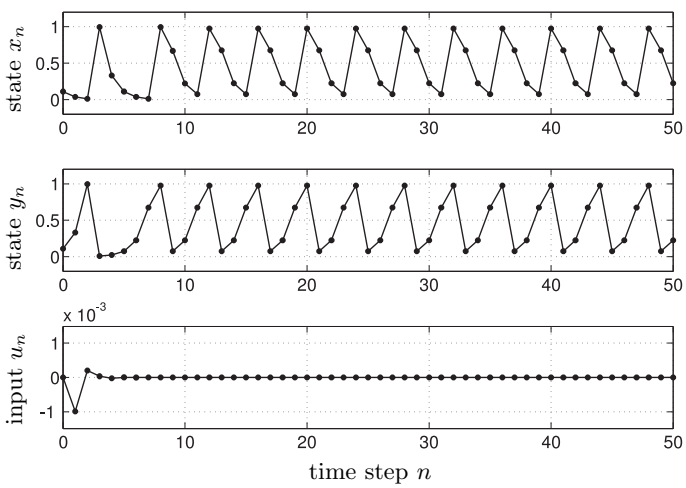

Fig. 8. Stabilization of a 4-periodic orbit embedded in a Smale horseshoe map; initial condition $(x_0, y_0) = (1/9, 1/9)$; design parameter $k = 5, l = 2$

6. CONCLUSION

In this paper, for a class of discrete-time systems that are topologically conjugate to symbolic dynamics, we proposed a control method to stabilize periodic orbits. We also showed application examples of the proposed control method, which were a one-dimensional control system for a population dynamics represented by a Logistic map and a two-dimensional control system with one input for the Smale horseshoe map. This is a new attempt to design control systems by using symbolic dynamics systematically in the sense that one estimates the magnitude of control inputs and analyzes the Lyapunov stability. The proposed control method can stabilize any periodic orbits with arbitrarily small inputs without switching the control law from targeting to local stabilization, and can ensure the robustness against noise by choosing the design parameter suitably. It is difficult with the conventional state space approaches to accomplish the stabilization like this, showing the effectiveness of the use of symbolic dynamics.

Applying theoretical results in terms of symbolic dynamics to the control system design may allow us to simultaneously accomplish the local stabilization and global targeting by small inputs for a wide class of complex systems. To generalize the proposed method, we need to investigate more practical situations such as cases in which systems are higher dimensional and the number of control variables is restricted. For the former case, high dimensional symbolic dynamics [9, 15] should be introduced, where multi-dimensional arrays of symbols rather than one-dimensional sequences are treated. Although we considered the latter problem for a simplified system in the previous section, careful geometric analysis for the dynamics in the state space will be required for general systems. Some concepts in control theory field such as accessibility and reachability may give us some hints. It is one of the main future works to characterize the possibility of desired changes in one- or multi-dimensional symbolic dynamics by a small number of degree-of-freedom of control.

The evaluation for the computational cost for calculating control inputs in our approach is also needed because it will increase as the governing equation becomes complex. The OGY method for the local stabilization just requires systems linearized around each periodic points. This low computational burden is one of its advantages. While our approach covers the global targeting and the control law is uniform even for different periodic orbits, we have to refine the proposed method so that the calculation cost is reasonable, which is another future work.

(Received June 21, 2014)

REFERENCES

[1] G. D. Birkhoff: Dynamical Systems. American Mathematical Society, New York 1927. DOI:10.1002/zamm.19280080636

[2] E. M. Bollt and M. Dolnik: Encoding information in chemical chaos by controlling symbolic dynamics. Phys. Rev. E *55* (1997), 6, 6404–6413. DOI:10.1103/physreve.55.6404

[3] N. J. Corron and S. D. Pethel: Experimental targeting of chaos via controlled symbolic dynamics. Phys. Lett. A *313* (2003), 192–197. DOI:10.1016/s0375-9601(03)00754-0

[4] C. M. Glenn and S. Hayes: Targeting Regions of Chaotic Attractors Using Small Perturbation Control of Symbolic Dynamics. Army Research Laboratory Adelphi MD 1996, No. ARL-TR-903.

[5] J. Hadamard: Les surfaces à curbures opposés et leurs lignes géodesiques. J. Math. Pure Appl. *5* (1898), 27–73.

[6] S. Hayes, C. Grebogi, and E. Ott: Communicating with chaos. Phys. Rev. Lett. *70* (1993), 20, 3031–3034. DOI:10.1103/physrevlett.70.3031

[7] Y.-C. Lai: Controlling chaos. Comput. Phys. *8* (1994), 1, 62–67. DOI:10.1063/1.4823262

[8] N. Levinson: A second order differential equation with singular solutions. Ann. of Math. (2) *50* (1949), 1, 126–153. DOI:10.2307/1969357

[9] D. Lind: Multi-dimensional symbolic dynamics. In: Symbolic Dynamics ans its Applications (S. G. Williams, ed.), Proc. Symp. Appl. Math. *60* (2004), 61–80. DOI:10.1090/psapm/060/2078846

[10] R. M. May: Simple mathematical models with very complicated dynamics. Nature *261* (1976), 459–467. DOI:10.1038/261459a0

[11] M. Morse and G. A. Hedlund: Symbolic dynamics. Amer. J. Math. *60* (1938), 815–866. DOI:10.2307/2371264

[12] J. Moser: Stable and Random Motions in Dynamical Systems. Princeton University Press, 1973.

[13] E. Ott, C. Grebogi, and J. A. Yorke: Controlling chaos. Phys. Rev. Lett. *64* (1990), 11, 1196–1199. DOI:10.1103/physrevlett.64.1196

[14] C. Robinson: Dynamical Systems: Stability, Symbolic Dynamics, and Chaos. CRC Press, 1999.

[15] E. A. Robinson, Jr.: Symbolic dynamics and tiling of $\mathbb{R}^d$. In: Symbolic Dynamics ans its Applications (S. G. Williams, ed.), Proc. Symp. Appl. Math. *60* (2002), 81–120. DOI:10.1090/psapm/060/2078847

[16] S. Smale: Diffeomorphism with many periodic points. In: Differential and Combinatorial Topology (S. S. Cairns, ed.), Princeton University Press 1963, pp. 63–80.

[17] S. Wiggins: Introduction to Applied Nonlinear Dynamical Systems and Chaos. Springer, 1991. DOI:10.1007/978-1-4757-4067-7

Masayasu Suzuki, 7-1-2 Yōtō Utsunomiya Tochigi, 3218585. Japan.
e-mail: ma-suzuki@ieee.org

Noboru Sakamoto, Furo-cho Chikusa-ku Nagoya, 4648603. Japan.
e-mail: sakamoto@nuae.nagoya-u.ac.jp